POLITECNICO DI TORINO
Repository ISTITUZIONALE

Intra-PON communication based on DSCM coherent-PON for ultra-low latency 5G/6G X-haul services

Original
Intra-PON communication based on DSCM coherent-PON for ultra-low latency 5G/6G X-haul services / Al Zoubi, S., Galardini, A., Gaudino, R.. - In: JOURNAL OF OPTICAL COMMUNICATIONS AND NETWORKING. - ISSN 1943-0620. - 18:5(2026), pp. 442-453. [10.1364/jocn.578877]

Availability:
This version is available at: 11583/3010850 since: 2026-08-06T07:56:20Z

Publisher:
Optica Publishing Group

Published
DOI:10.1364/jocn.578877

Terms of use:

This article is made available under terms and conditions as specified in the corresponding bibliographic description in the repository

Publisher copyright

(Article begins on next page)

08 November 2026

JOURNAL OF
Optical Communications
and Networking

Intra-PON communication based on DSCM coherent-PON for ultra-low latency 5G/6G X-haul services

Safana Al zoubi,[1,*] Alessandro Galardini,[2] and Roberto Gaudino[1]

[1]Dipartimento di Elettronica e Telecomunicazioni, Politecnico di Torino, Torino, Italy
[2]Consorzio TOP-IX, Torino, Italy
*safana.alzoubi@polito.it

Received 12 September 2025; revised 6 November 2025; accepted 20 March 2026; published 16 April 2026

Future passive optical networks (PONs) are expected to support the ultra-high bitrates and extremely low-latency requirements of X-haul networks. In parallel, many research groups and standardization bodies are investigating PON transmission solutions for 100+ Gbps per wavelength (very high speed PON or VHSP), considering also the introduction of coherent transmission technologies in PON. Building on these two trends, we propose and analytically investigate simple physical modifications to the standard PON infrastructures to enable direct all-optical ONU-to-ONU communications, showing their rationale for X-haul. We introduce both intra- and inter-PON ONU-to-ONU all-optical configurations and assess their impact on optical distribution network (ODN) loss, considering current and future-compliant transceivers. We focus in particular on coherent PON based on digital subcarrier multiplexing (DSCM), which is one of the solutions currently investigated by the ITU-T for VHSP. Our analysis shows that, under reasonable assumptions for future PON-complaint DSCM-based transceivers, the proposed architectures can support 40 km ONU-to-ONU links with an additional allowed loss margin of about 1.3 dB beyond the 29 dB N1 PON class limit, and one ONU to four ONU connections with only 2 dB of extra margin. Furthermore, the proposed architectures achieve significant latency reductions, making them suitable for future low-latency split- and service-based transport requirements. © 2026 Optica Publishing Group under the terms of the Optica Open Access Publishing Agreement

https://doi.org/10.1364/JOCN.578877

1. INTRODUCTION

Recent research and industrial efforts toward future passive optical network (PON) generations aim to support a wide range of service types, including fiber-to-the-home (FTTH), fiber-to-the-enterprise (FTTE), and fiber-to-the-antenna (FTTA), using different X-hauling approaches. To achieve this, these efforts are considering coherent transmission and its digital subcarrier multiplexing (DSCM) variant [1,2], new optical access architectures [3], the potential convergence between metro and access networks [4], and even wavelength division multiplexing (WDM) in access networks [5]. In particular, a working group in the International Telecommunication Union (ITU-T) is currently leading an initiative addressing all these technical options under the very high speed PON (VHSP) initiative. If and when a technological jump from intensity modulation-direct detection (IM-DD) traditional PONs toward single- or multi-carrier coherent transmission occurs, it will enhance the overall network capacity, reach, and flexibility, enabling more unified architectures from metro to access. In particular, point-to-multipoint transmission based on DSCM has shown strong potential to deliver high spectral efficiency and dynamic bandwidth management in access networks [6–8]. This is specifically relevant as operators seek scalable solutions to accommodate increasing traffic demands while maintaining cost-efficiency, operational simplicity, and technology backward compatibility.

Given these foreseen increases in PON bitrate capabilities, combined with its widespread geographical coverage, it is increasingly regarded as a strong candidate for supporting X-haul services, including front-haul, mid-haul, and back-haul [3]. This is particularly important and challenging as the transition to beyond 5G (B5G) and future 6G networks introduces stringent requirements for higher bitrates, massive densification, and ultra-low-latency services [9], with the diverse range of provisioned 6G use cases, such as mixed reality, autonomous mobility, and AI-driven communication, further pushing the need for cost-effective, dynamic, and high-performance transport solutions.

Latency is especially crucial to consider and manage when deploying PON for X-haul services and, particularly, for some of the future aforementioned new applications. Multiple research efforts have addressed this challenge in conventional

PONs [10], mainly along two directions. The first focuses on mitigating latency caused by PON time-division multiple access (TDMA)-based shared infrastructure, through advanced bandwidth allocation algorithms, such as cooperative schemes between the radio and access segments, that optimize upstream scheduling and reduce end-to-end delay [11]. A second (and much more recent) direction targets architectural latency reduction by enabling intra-PON communication, which allows direct communications between optical network units (ONUs) within the same PON tree, thereby avoiding the need to traverse the optical line terminal (OLT) [3,12]. The concept of intra-PON communication is introduced here and will be further elaborated in Section 3 (see Fig. 2). This approach reduces physical distance and enables emerging use cases where multiple ONUs serve distributed small cells, while computing resources are centralized at a macro cell, leading to improved coordination and resource efficiency.

Building on the concept of all-optical direct ONU-to-ONU communication as a means to support low-latency X-haul services, and considering the solution proposed in the literature on coherent PONs using DSCM, we propose simple physical modifications to existing PON infrastructures enabling direct ONU-to-ONU communications. The proposed architectures, schematically illustrated later in Figs. 3 and 7, allow both dynamic and flexible intra-PON communication (between ONUs located within the same PON tree) and inter-PON communication (between ONUs in different PON trees that are all-optically connected), respectively. Our proposal is applicable in both coherent PON and converged metro + PON scenarios facilitating all-optical, direct ONU-to-ONU connections. A key feature of the design is the use of asymmetrical splitters with extremely low insertion loss, which minimizes the impact of the architectural modifications on the overall PON distribution loss. We assess the feasibility of these architectures in terms of power budget and compare their latency performance with that of benchmark configurations.

The remainder of this paper is organized as follows. Section 2 provides an overview of the future radio network requirements based on X-hauling in terms of required bitrates and, in particular, latency in order to explain the rationale for a future evolution toward ONU-to-ONU all-optical communications. Section 3 describes the coherent intra-PON architectures and presents a first-order power budget analysis. Section 4 extends the application of the same concepts toward converged metro and PON inter- and intra-PON communication schemes, including again a preliminary power budget assessment. Section 5 evaluates the latency reduction achieved through the proposed inter- and intra-PON communications. Finally, Section 6 concludes the paper and outlines directions for future research.

2. FUTURE RADIO REQUIREMENTS AND X-HAULING TRENDS

In this section, we discuss future X-haul requirements to justify the need for ultra-high bitrate, flexible, and dynamic access networks with decreased latency compared to current solutions. This need arises from the fact that future X-haul networks are expected to undergo a substantial increase in bitrate requirements, along with more stringent latency constraints, to meet the demands of B5G and 6G goals [9,13]. We will show in this section that the resulting bitrate and latency requirements are not only highly demanding but also highly variable across different services and deployment scenarios.

Transport bitrate requirements are primarily determined by the actual radio physical layer request (such as the RF allocated band, as we will describe later) and on the selected functional split, which defines how baseband processing tasks (from the control layer to the physical layer) are distributed among the central unit (CU) and the distributed unit (DU), as specified by the 3rd Generation Partnership Project (3GPP) [14–16]. In the traditional 3GPP evolution, this CU/DU split represents the main architectural disaggregation. By contrast, Open RAN (O-RAN) also introduces the radio unit (RU) and further extends this concept, driving a significant architectural shift by embracing openness and disaggregation between RU, DU, and CU components. For further information about functional split in a RU, DU, and CU architecture, we suggest the reader to refer to the tutorial given in [16]. In the following, we briefly mention some features that are specifically relevant to the rest of our paper. The so-called "higher-layer splits," such as option 2, decentralize the radio processing, thus reducing traffic load on transport links and relaxing latency constraints, but requiring more complex antenna sites and allowing less coordination. In contrast, lower-layer splits, such as option 8, simplify antenna sites and enable better coordination across the full protocol stack, but impose higher bitrate demands and stricter latency constraints on the optical network. Furthermore, the X-haul bitrate is dependent on the air interface specifications, including factors such as the radio bandwidth, orthogonal frequency division multiplexing (OFDM) symbol configuration, number of multiple-input multiple-output (MIMO) layers, antenna ports, modulation and coding schemes, in-phase and quadrature (IQ) bitwidth, and peak air interface data rates. To illustrate these dependencies, Table 1 presents two scenarios of advanced X-haul bitrate requirements reflecting the 5G and 6G-basic along with the latency constraints associated with standard 3GPP radio split options.

As a first scenario, we consider a 5G X-haul downlink with a radio bandwidth of 100 MHz, 256-QAM modulation,

Table 1. Different Functional Split Options Proposed by 3GPP with Their Latency and Bitrate Requirements for the Two Deployment Scenarios Considered in Our Paper, Indicated as "5G" [14,15] and "6G-Basic" [9][a]

Functional Split #	Split-Specific Latency (ms)	5G Bitrate (Gbps)	6G-Basic Bitrate (Gbps)
1	10	∼4	16
2	1.5–10	∼4	∼16
4	0.1	4	16
6	0.25	4.2	∼16
7.3	0.25	4.2	50.4
7.2	0.25	22.2	86.7
7.1	0.25	86.1	688.25
8	0.25	157.3	1.25 Tb/s

[a]See text for more details.

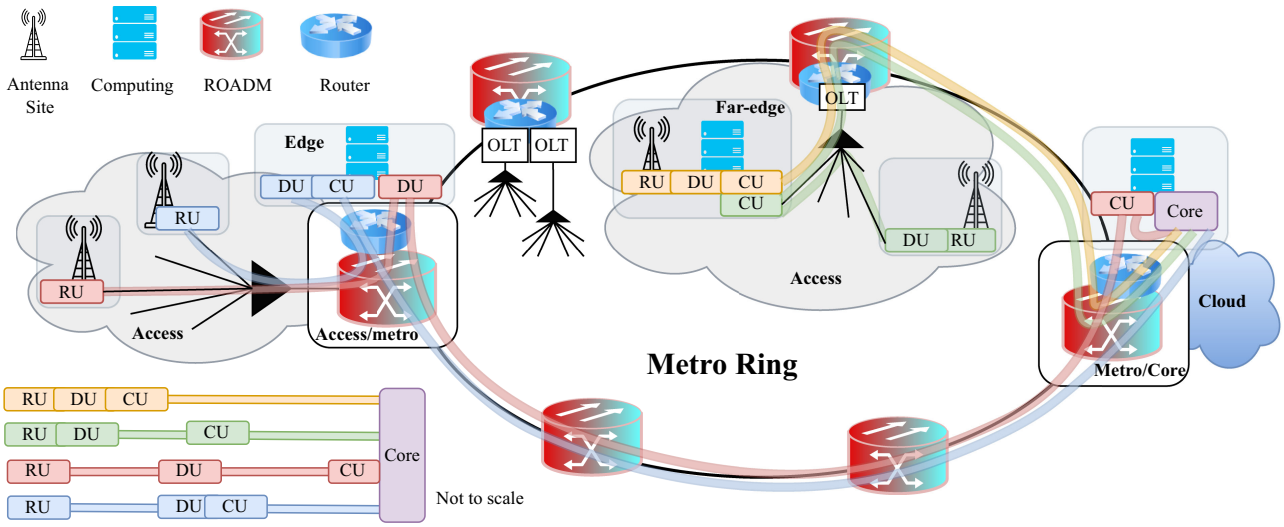

Fig. 1. Example of an optical network supporting B5G and 6G flexible functional splits. The different possible logical paths are indicated using different colors.

32 antenna ports, 8 MIMO layers, IQ bitwidth of 2×16 bits, 14 OFDM symbols, and 1200×5 radio subcarriers. As a second, even more advanced scenario, which we will indicate as "6G-basic," we consider a wider radio bandwidth and an increased number of antennas: a radio bandwidth equal to 400 MHz and 64 antenna ports, while keeping the other parameters unchanged [9,14]. As a preliminary observation, Table 1 shows that for our considered 5G and 6G scenarios, some split options, and in particular Split 8 (i.e., the "traditional" digitized front-hauling used in the CPRI initiative), have exceedingly high bitrate requirements and are clearly not feasible even in next-generation VHSP, while a reasonable compromise is likely using one of the 7.x split options.

Latency constraints, on the other hand, depend not only on the selected functional split, as illustrated in Table 1, where low-layer splits typically require a one-way propagation delay of less than 250 µs, but also on the end-to-end latency requirements of supported services for specific radio use cases, i.e., service-based latency. The latter refers to the total end-to-end delay experienced from the RU through the DU and CU up to the core network gateway. For instance, 3GPP defines ultra-reliable low-latency communications (URLLC), where use cases such as tactile interaction, motion control, and industrial collaborative control require end-to-end latencies of 0.5 ms, 1 ms, and under 2 ms, respectively [3]. These dual constraints highlight the critical role of the transport network, where achieving latency on the order of a few hundred microseconds is required to satisfy both the split-related and the service-specific latency requirements. For example, the O-RAN working group 9 (WG9) in [17] presents use case latencies specifically for the function split 7.2x between the RU and DU, with requirements of less than the 3GPP-defined 250 µs, such as the latency class "High75," which specifies 75 µs delay to support full New Radio (NR) performance with fiber lengths of up to 10 km, and "High100," which specifies 100 µs for standard NR performance with fiber lengths of up to 10 km.

In parallel, future radio approaches enable flexible deployment of virtualized network functions at various network locations, such as the antenna, far edge, edge, or cloud site, to support different radio use cases. Figure 1 schematically shows some of the possible options that we will address in the rest of the paper. This deployment flexibility enables dynamic functional splitting, thus supporting the optimization of latency, capacity, energy efficiency, and system complexity by dynamically assigning processing functions within the RAN.

Given these evolving demands and dynamic architectures, conventional fixed point-to-point fiber-based X-haul solutions may soon fail to scale economically, particularly under the increased cell density anticipated in the B5G and 6G scenarios. Instead, it may likely happen that the widespread geographical availability of optical access based on PON (it is estimated that in 2025 more than 1 billion PON terminations were available worldwide) and the aforementioned increase in PON bitrates to more than 100 Gbps per wavelength (see, for instance, the ITU-T VHSP initiative) may shift X-hauling to PON shared infrastructure, offering a more scalable and cost-effective solution to accommodate highly dynamic and demanding X-haul traffic. Anyway, as mentioned in the introduction, traditional TDMA-based PON solutions may be critical in terms of latency requirements, thus justifying the current research toward alternative solutions. Moreover, flexibility in future deployments serves as a key enabler for network virtualization and software-defined network (SDN) orchestration.

3. PROPOSED ONU-TO-ONU ARCHITECTURES ENABLED BY DSCM-BASED COHERENT PON

To address the low latency and high bitrate requirements outlined in Section 2, we propose intra-PON direct ONU-to-ONU communication using DSCM-based coherent transmission for B5G and 6G networks. Figure 2 shows a simple physical illustration of the intra-PON concept, contrasting a conventional PON, where ONU-to-ONU traffic passes through the central OLT, with the proposed approach, in which a direct optical link is established between ONUs. It is worth noting that intra-PON communication also occurs at

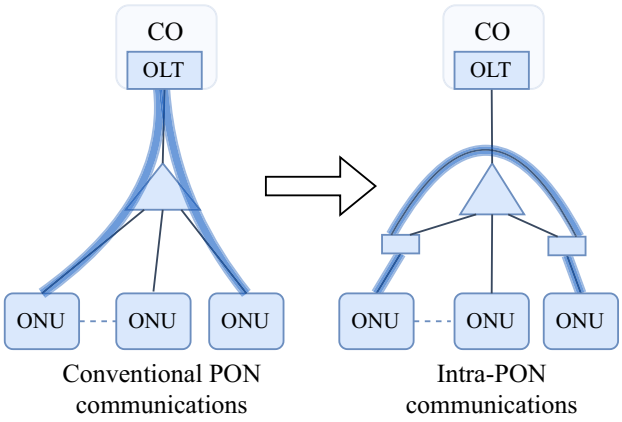

Fig. 2. Simplified illustration of ONU-to-ONU communications within a PON tree: conventional PON versus intra-PON. CO, central office.

Layer 2 in various PON generations and is commonly referred to as hairpin or intra-PON forwarding. In this configuration, the OLT forwards traffic received from one ONU directly to another ONU within the same PON, without passing it to higher layers of the network [18]. However, this still requires optical–electrical–optical (O-E-O) conversion within the OLT with the related queuing delay in the electronic switch and may involve additional fiber distances compared to the proposed setups, particularly in long-reach PON and/or metro-access architectures.

In the following, we present a more detailed illustration of the PON physical architecture, along with the proposed modifications to enable all-optical links between ONUs, followed by a first-order analysis of the power budget considerations to support these connections.

A. Proposed Physical Architectures

Figure 3 illustrates the typical shared PON infrastructures, featuring a single-stage splitting configuration in subfigures (a) and (b) and a two-stage splitting arrangement in (c) and (d) (both options are today very common in PON deployments). The same figure also shows the simple modifications to the optical distribution network (ODN) that we are proposing to enable novel all-optical ONU-to-ONU intra-PON connections, which are based on the addition of optical splitters and new fibers. We now go into the details of the four possible configurations that we address in this section. In the remainder of this paper, asymmetrical splitters are referred to as taps, while symmetrical splitters are denoted as splitters.

We start with the proposal shown in Fig. 3(a) for a single-stage splitter PON. Here, an ONU-to-ONU intra-PON communication link is established by adding inside the splitter cabinet two properly placed asymmetrical splitters (taps) and a short fiber patch-cord. We point out that this proposal would require minimal modification in the ODN and, in particular, just a manual modification inside the street cabinet, without any other modifications outside the cabinet.

This first configuration, shown in Fig. 3(a), allows us to preserve the "traditional" connectivity with the main OLT while enabling a direct all-optical path between the two target ONUs. In particular, DSCM-based coherent PON is particularly suitable to achieve this goal: subcarriers (SCs) can be distinctly assigned, ensuring that SCs allocated for intra-PON communication differ from those used for regular PON transmissions. Moreover, subcarriers should not superimpose spectrally for both upstream (US) and downstream (DS), which is known as subcarrier interleaving. This is because, in contrast to metro coherent systems where two separate fibers are used for US and DS transmission, PON systems employ single-fiber bidirectional transmission. Therefore, in this study, circulators are deployed at both the OLT and ONU to separate the DS and US signals propagating along the same fiber, combined with subcarrier interleaving (as experimentally demonstrated in [19]) to mitigate back-reflections. However, research efforts are still ongoing on full-duplex DSCM (conceptually similar to single-carrier coherent PON systems) through approaches such as employing dual wavelengths or other network modifications [20]. For instance, assuming a DSCM using 16 subcarriers and an arbitrary SC numbering intended solely for illustrative purposes, the lower inset in Fig. 3(a) shows a possible SC allocation where SCs 1–4 can be used for US regular traffic (dark gray color) and SCs 5–10 for DS regular traffic (light gray color). In this illustrative allocation, regular ONUs are assigned SCs 1–10; however, since DSCM supports flexible bandwidth allocation using time-frequency division multiple access (TFDMA) [21,22], each ONU can be assigned any number of subcarriers (e.g., 2, 4, or more) depending on its transceiver design and its bandwidth requirements. In existing implementations, such as in [6], ONU DSCM transceivers have been demonstrated with up to four SCs per direction without time-division multiplexing, while ongoing research continues to investigate more scalable and flexible configurations. The remaining SCs from 11 to 16 can be used for our new proposal. In particular, assuming the DU is located at a different site than the RU, a bidirectional communication between their ONUs can be established using distinct subcarriers, namely, SCs 13 and 14, to represent US and DS transmission, respectively. Concurrently, each ONU maintains independent communication with the OLT via separate SCs, such as SCs 11 and 12 for DU-ONU to OLT and SCs 15 and 16 for RU-ONU to OLT. The subcarriers from 11 to 16 are assumed to be exclusively assigned in the frequency domain and are not time-shared. Throughout this paper, the RU–DU connection denotes the link between their ONUs, while the "RU/DU–OLT connection" denotes the link from each ONU to the OLT. It is important to note that intra-PON communications are also received by the OLT, providing additional flexibility in SC allocation and scheduling according to temporal data requirements. This is one of the advantages of our proposed approach compared to other solutions, such as point-to-point or coherent/nested PON alternatives. For instance, to connect two ONUs—or more generally, two points located near PON terminations—there are two possible approaches: (1) deploying new point-to-point fiber links, which is costly and contradicts our goal of avoiding additional fiber infrastructure, or (2) modifying the existing PON with an overlay connection, either coherent or through another nested PON (as described in [3]). This second approach enables ONU-to-ONU communication but requires an additional

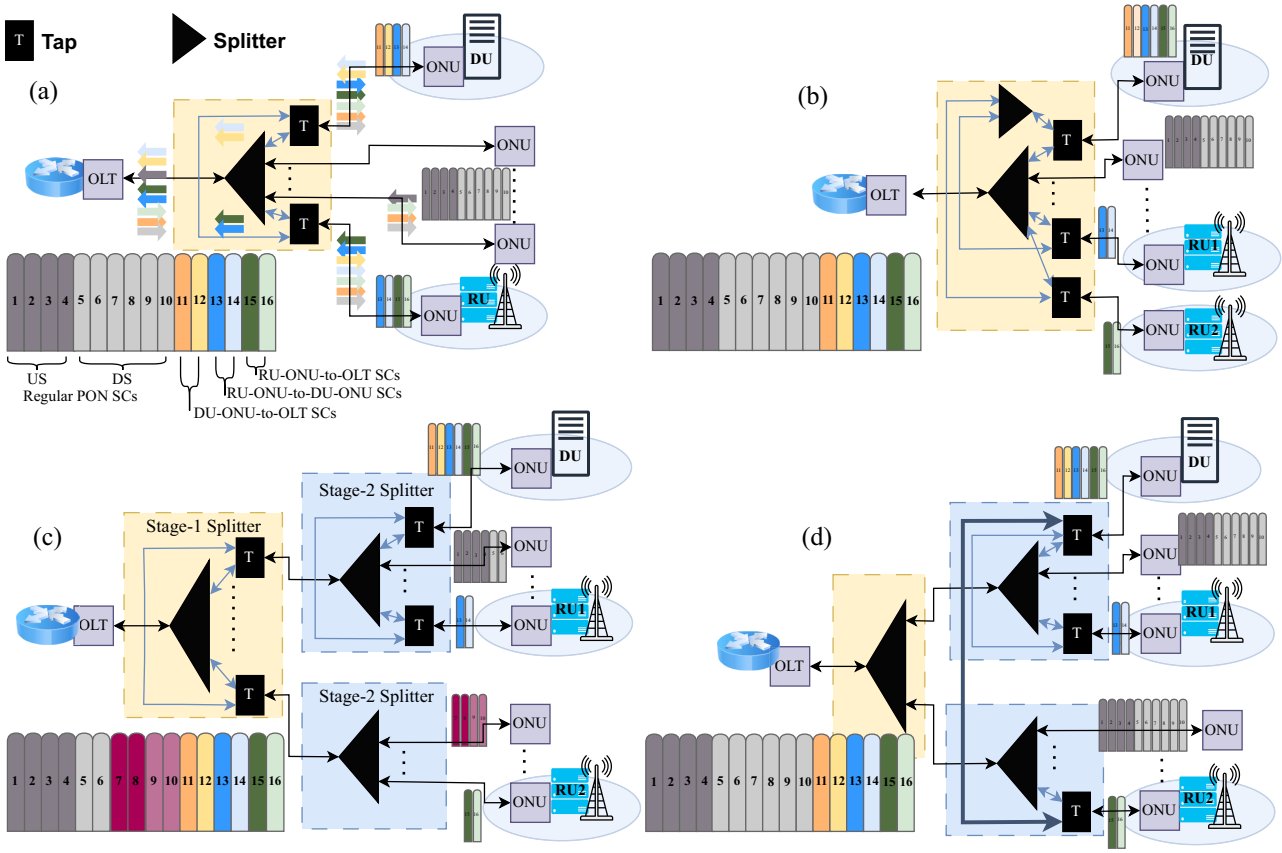

Fig. 3. Proposed intra-PON communication architectures for coherent DSCM-PON with one or two stages of splitting: (a) one-to-one connection with a single-stage splitter, (b) one-to-few connection with a single-stage splitter, (c) one-to-few connection with two stages of splitting by modifying the stage-1 splitter, and (d) one-to-few connection with two stages of splitting by adding a new fiber link between stage-2 cabinets. Tap, asymmetrical splitter; splitter, symmetrical splitter.

wavelength and transceiver to maintain the OLT connection. Furthermore, if the demand on one link varies over time, the established connection cannot be flexibly reused on the other.

One important aspect to consider is the coexistence of the proposed DSCM coherent-PON communication with "legacy" IM-DD PON standards (such as GPON, XG-PON, NG-PON2, and 50-GPON). As shown in detail in [6], a DSCM coherent-PON can be implemented as an overlay on existing PON infrastructure just assuming operation on separate wavelengths with a proper wavelength compatibility plan. In fact, if a different wavelength band is assigned to the DSCM coherent-PON (as for sure the ITU-T VHSP initiative will force), the newly established intra-PON links do not interfere with the existing connections of regular legacy ONUs.

A second architecture, implementing an example of one-to-few intra-PON communication, is presented in Fig. 3(b), where we show how two RUs can establish bidirectional communication with one DU by adding three taps and a splitter. In fact, the architecture can be extended to more than two RUs, as we will discuss later in the link budget analysis. Here, we focus on only two RUs for simplicity in the schematic. Similar to the previous case shown in Fig. 3(a), the required modification acts only in the main PON splitter cabinet, and it enables the RU1 and RU2, located at different sites, to intra-communicate to DU at another site while maintaining their connection to the OLT, provided that SCs are properly planned. In this one-to-few setup, the value of the splitter number of output ports (ranging from a 1:2 to a 1:N) determines the number of ONUs connected to the DU. For example, a 1:2 splitter in this figure facilitates intra-PON communication between the DU and two other ONUs. Importantly, this modification to the PON infrastructure does not affect the links of other ONUs, making it a viable solution for establishing new, flexible connections that can coexist with current and legacy PON standards.

Extending this concept further, we also show that intra-PON communications can also be established in PON deployments where two stages of splitting are present. In such architectures, connecting two ONUs that branch from the same stage-2 splitter cabinet follows the same approach as in the single-stage case, as illustrated in Figs. 3(c) and 3(d) for the connection between the DU and RU1. This is achieved by adding two taps linked by a short-length fiber inside the stage-2 cabinet. On the contrary, for ONUs connected to different stage-2 cabinets, such as the DU and RU2 in Figs. 3(c) and 3(d), two approaches are possible. The first, shown in Fig. 3(c), involves modifying the stage-1 splitter to interconnect the two level-2 PON branches by adding new taps in the stage-1 splitter cabinet and connecting the two stage-2 branches by a short-length fiber. In this case, since the two stage-2 branches are interconnected, SC allocation must be

distinct not only between the target ONUs but also across the branches to avoid interference and ensure proper intra-branch communication. The second approach, illustrated in Fig. 3(d), is to connect the two stage-2 cabinets via a dedicated point-to-point fiber in addition to the added taps, although this solution is generally not preferred due to the associated cost of deploying a new fiber.

It should be noted that, in a two-stage splitter architecture, coexistence with legacy PON wavelengths is feasible only in the second configuration [i.e., Fig. 3(d)]. In the first configuration [i.e., Fig. 3(c)], signals from intra-connected stage-2 branches will interfere because they occupy the same frequency spectrum.

B. Link Budget First-Order Analysis

To assess the feasibility of the proposed intra-PON communications in DSCM-based coherent PON, three main factors must be taken into account.

- First, it is important to minimize any modifications to the physical architecture and power budget of the original PON ODN, ensuring backward compatibility and ease of integration with existing systems.
- A second consideration involves maintaining the power difference between the SCs within a defined threshold, as significant imbalance at the receiver can lead to performance penalties, as shown in [6,8]. Here, we consider that the maximum allowed power difference between SCs at a given receiver is 10 dB, as reported in [6].
- Third, the newly established links must maintain a sufficient power budget to support reliable communication. According to the ITU-T PON standards, the N1 optical path loss (OPL) class requires a power budget of 14–29 dB, and up to 20–35 dB for the E2 class. Consequently, if and when DSCM transceivers are deployed in future PONs, they should comply with at least the PON N1 OPL class requirement of 29 dB defined by ITU-T. Experimental results provide context for the capabilities of current prototype DSCM transceivers suitable for PON applications, such as in [6], where optical path loss measurements were conducted for DSCM transmission in a point-to-multipoint setup coexisting with legacy PONs using a commercial state-of-the-art transceiver. The study reported a maximum uplink OPL of 25.6 dB at a wavelength of 1544 nm, with a transmitted power of 1.2 dBm, 40 km of fiber, and a 200 Gbps bitrate (both directions). In [23], a different transceiver and experimental configuration achieved power budgets of 30 dB downstream and 33 dB upstream. While these results represent the current state of the art for DSCM transceivers, the technology is still under research and has not yet reached its full maturity.

Therefore, we begin our PON power budget analysis by assuming that the future DSCM transceivers comply with the ITU-T N1 class, allowing for an OPL of 29 dB. We then examine how the addition of taps affects this loss and determine the required additional transceiver margin (in dB) to enable intra-PON communication. A key consideration in this context is the insertion loss introduced by the taps. The split ratios used are taken from [24] and summarized in Table 2, where we list asymmetrical splitting options, as these will later be shown to offer particular advantages in the proposed architecture.

Table 2. Split Ratios and Corresponding Insertion Loss

Split Ratio	Insertion Loss	Split Ratio	Insertion Loss
50/50%	3.5/3.5 dB	20/80%	7.8/1.3 dB
40/60%	4.6/2.7 dB	10/90%	11/0.75 dB
30/70%	5.9/1.9 dB	5/95%	14.5/0.4 dB

We start by analyzing the one-to-one setup shown in Fig. 3(a). Figure 4 illustrates the power loss as a function of the split ratio of the added taps for both ONU-to-OLT and ONU-to-ONU communication. We consider that both of the added taps employ the same split ratio (x_1/x_2), where x_1 corresponds to the new link and x_2 to the main path to the OLT, and we vary them simultaneously. The feeder fiber (i.e., before the splitter) is assumed to be either 10 or 0 km, while the distribution fiber in all paths after the splitter is assumed to be either 10 or 20 km, respectively. Thus, the fiber distance between ONUs (from an ONU to the splitter cabinet and then to another ONU) amounts to either 20 or 40 km, respectively. The case of 0 km feeder fiber represents the worst-case scenario, corresponding to the maximum ONU-to-ONU distance of 40 km. For ONU-to-OLT communication, we consider the starting point corresponding to the mandatory compliance budget of 29 dB, plus the loss from the added tap, i.e., 0.4 dB for the lowest split ratio 5/95%. For ONU-to-ONU communication with 20 km of fiber, the starting point is the sum of the 2 × 14.5 dB loss from two taps and the fiber loss. Figure 4 clearly shows the relevance of properly selecting the splitting ratio in the two additional taps. In our opinion, the optimal split ratio is where the two loss curves intersect, representing the minimum additional margin required to support both ONU-to-OLT (PON) and ONU-to-ONU (intra-PON) communication. For the 20 km case, this occurs around a 10/90% split ratio, requiring an extra-margin equal to 0.75 dB, meaning the transceiver should support a budget of 29.75 dB to be considered as compliant with intra-PON communication. For the 40 km case, the optimal split ratio is 20/80%, which

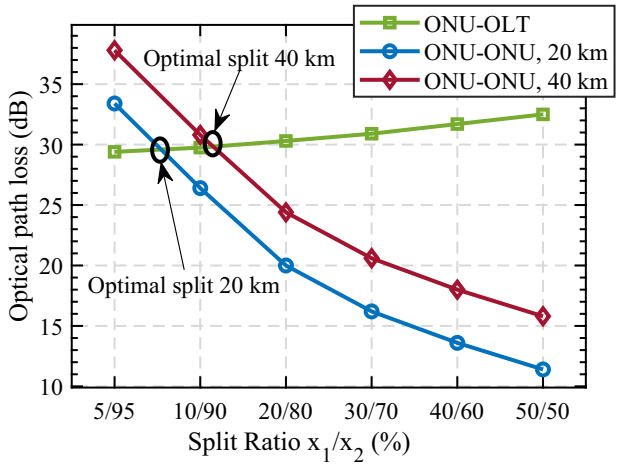

Fig. 4. Power loss as a function of the tap split ratio in a one-to-one intra-PON connection with a single-stage splitter.

Table 3. Optimal Split Ratio and the Corresponding Margin (in dB) Required to Enable Both PON and Intra-PON Communications in a One-to-Few Configuration, as a Function of ONU-to-ONU Fiber Length and the Number of Connected ONUs

		Connected ONUs		
Fiber Length	**Metric**	**Two**	**Three**	**Four**
20 km	Split (%)	10/90	20/80	20/80
	Margin (dB)	29.9	30.3	30.3
40 km	Split (%)	20/80	20/80	30/70
	Margin (dB)	30.3	30.3	30.9

requires an additional margin of 1.3 dB. For shorter distribution fibers (as is often the case in practical deployments), even more asymmetric splitting ratios would be optimal, since the fiber loss on the ONU-to-ONU path would be lower, thus creating even lower extra-margin requirements.

Considering the one-to-few architecture with a single-stage splitter shown in Fig. 3(b), the optimal split ratio and the required extra margin in a future-compliant transceiver are presented in Table 3. Here, we consider the one-to-few connection as one ONU connecting to two, three, or four ONUs, and the total fiber length from ONU to ONU (i.e., ONU-splitter cabinet-ONU) to be either 20 or 40 km. As shown in Fig. 3(b), the intra-PON communication is achieved by a tap followed by a splitter (1:2, 1:3, or 1:4 symmetrical splitter), corresponding to equal insertion losses of 3.5, 5.6, and 7.0 dB, respectively [24,25]. The table shows that regular PON and intra-PON communications can be achieved with an additional 2 dB margin even for a fiber length of 40 km and a 1-to-4 ONU configuration. It should be noted that, although we illustrated ONU-to-ONU connections up to four, this number represents only simultaneous PON and intra-PON communications, while the total number of regular ONUs can remain high and consistent with typical PON deployments, such as a 64-ONUs PON in which only four of them are supporting DU/RU X-haul. Moreover, the number of these connections can be increased, which would consequently lead to higher losses for the considered ONUs. However, given that a typical PON tree spans less than 20 km, the number of radio cells requiring intra-PON communication is expected to be significantly lower than the number of PON terminations; therefore, the presented example reflects the considered scenario.

After this preliminary and worst-case link budget analysis, we discuss in the following the proposed architectures in a more realistic statistical link budget analysis, a point of view motivated by the inherent variability of ODN loss and the need to understand the power differences between SCs at a given receiver. ODN loss in a PON generally depends on deployment factors such as fiber lengths and split ratios. In dense urban areas, PONs may feature short fibers and high split ratios concentrated in a single stage, while suburban deployments often involve two stages of splitting with longer fiber distances. A publicly available statistical characterization of ODN loss is presented in [26], based on an extensive set of measurements from the Orange installed FTTH customer base in France (several million PON terminations have been characterized in that study). The presented measured loss distribution can be approximated by a log-normal profile, with a median path loss of 23.4 dB, a first quartile (Q1) of 22 dB, and a third quartile (Q3) of 25 dB. Taking these factors into account, we evaluate the impact of the added taps' split ratios and their associated insertion losses on the overall PON loss. For this analysis, we consider two OPL thresholds: 25.6 as the current achievable OPL limit and 29 dB as the target defined by the PON N1 class.

Figure 5(a) presents the OPL analysis as a function of the power split ratios of the additional taps to the setup shown in Fig. 3(a), where a one-to-one intra-PON connection is established. Similar to Fig. 4, we assume that both taps employ the same split ratio (x_1/x_2), and we vary them simultaneously. The OPL median values for the links between ONUs to the OLT, the RU-to-OLT, and the DU-to-OLT are represented by black square points in Fig. 5. These points are shown with surrounding bars indicating the interquartile range (IQR), i.e., Q3–Q1, illustrating the distribution when the links follow PON statistics. These links are assumed to follow the median and IQR of the original PON, with an added loss attributed to the inserted taps. Additionally, the OPL of the new link between the RU and DU is calculated by summing the tap loss and the fiber propagation loss over 20 km. In this scenario, split ratios of 5/95, as well as 30/70 and higher, are considered infeasible due to the significant power difference between the new link and the other ones, as indicated by the power imbalance in

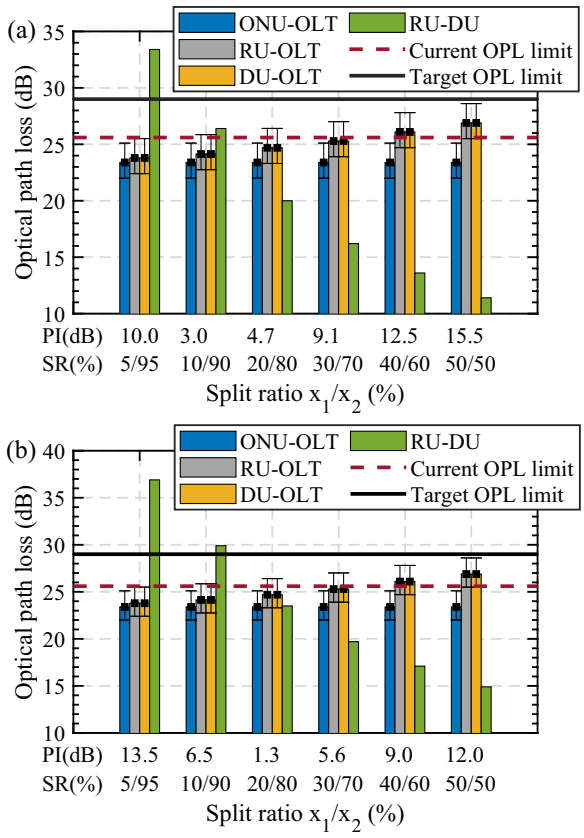

Fig. 5. Intra-PON power budget analysis for two communication scenarios: (a) one-to-one communication and (b) one-to-two communication, for different split ratio options for the added taps. The numbers shown below the figures denote the power imbalance corresponding to each split ratio. PI, power imbalance; SR, split ratio.

the figure, where this imbalance considers the median value when the link follows PON statistics. Conversely, split ratios of 10/90 and 20/80 are more suitable for maintaining the PON OPL below the thresholds and ensuring the power difference between SCs remains under 10 dB. It should be noted that this particular setup does not affect the OPL of regular ONUs, as reflected in the ONU-to-OLT loss across the span for the considered tap split ratios; consequently, the proposed architecture can be implemented as an overlay without impacting legacy PON systems.

For the case of one-to-few intra-PON communication, illustrated in Fig. 3(b), the splitter here is assumed to be a symmetrical 1:2 splitter, resulting in an insertion loss of 3.5 dB [24]. Additionally, the other taps involved are assumed to be identical and are varied simultaneously. Figure 5(b) illustrates the impact of the tap split ratios on the various links within the modified PON. As observed, the original ONU-to-OLT links remain identical to the previous case. In contrast, the OPL of the RU-to-OLT and DU-to-OLT links increases with higher split ratios, as more power is diverted to the newly established intra-PON links. The RU-to-DU link loss accounts for both the taps' insertion losses and a total fiber length of 20 km. As shown, split ratios of 5/95, as well as 40/60 and above, are considered not feasible due to the significant power imbalance between SCs. Split ratios of 10/90, 20/80, and 30/70 appear to be more suitable for enabling one-to-few intra-PON communication.

Alternatively, when considering two stages of splitting with the proposed architecture illustrated in Fig. 3(c), the PON deployment plays a crucial role in determining the feasibility of establishing intra-PON communication. In this analysis, we consider two RUs: the first RU (RU1), which belongs to the same stage-2 splitting branch as the DU (intra-stage), and the second RU (RU2), which belongs to a different stage-2 splitting branch from the DU (inter-stage). We evaluate the OPL for both links under two scenarios. The first scenario, whose results are shown in Fig. 6(a), consists of a 1:4 stage-1 splitter followed by a 1:16 stage-2 splitter, with fiber lengths of 10, 5, and 5 km representing the fiber from the OLT to the stage-1 splitter (feeder fiber), from the stage-1 splitter to stage-2 splitter, and from the stage-2 splitter to the ONU, respectively. The second scenario results, shown in Fig. 6(b), involve a 1:16 splitter followed by a 1:4 splitter, with fiber segments of 15, 4, and 1 km. These parameters are chosen to illustrate the feasibility of the proposed intra-PON communications in a two-stage splitting and to highlight the significant impact of specific network characteristics. In the intra-stage case, i.e., RU1 and DU, the link passes only through the newly added taps and a short fiber segment. On the other hand, in the inter-stage case, i.e., the connection between RU2 and the DU, the link experiences very high loss, as the signal passes through both stage-2 splitters. This loss is even greater in the first scenario (1:4 splitter followed by 1:16) compared to the second (1:16 splitter followed by 1:4), as the higher splitting occurs in stage-2. To compensate for this loss difference, the two added taps in the stage-2 splitter cabinet are fixed at a 5/95% split ratio, while the split ratio of the taps in the stage-1 splitter cabinet is varied simultaneously, and their impact on

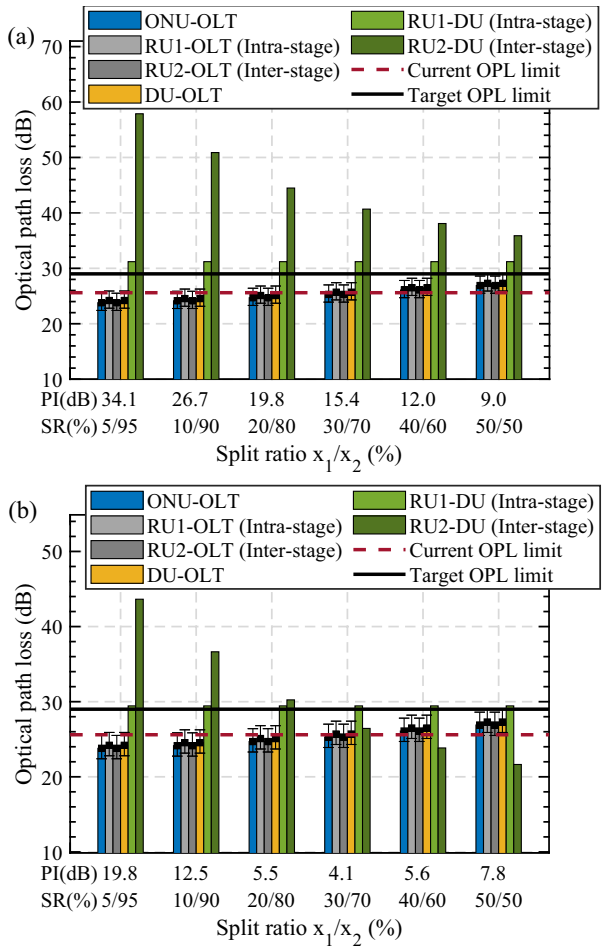

Fig. 6. Intra-PON power budget analysis for a two-stage PON splitting architecture: (a) 1:4 splitter followed by 1:16, with fiber segments of 10, 5, and 5 km; (b) 1:16 splitter followed by 1:4, with fiber segments of 15, 4, and 1 km. Intra-stage: RU in the same stage-2 branch as the DU. Inter-stage: RU in a different stage-2 branch from the DU. The values shown below the figures denote the power imbalance associated with each split ratio. PI, power imbalance; SR, split ratio.

the power budget is evaluated accordingly. As shown, intra-stage communication between RU1 and the DU is feasible in both scenarios, consistent with the results in Fig. 5(a), though it requires an additional margin of approximately between 0.5 and 2.2 dB beyond the 29 dB threshold. For the RU2-DU (inter-stage) link, however, the power imbalance relative to the other links is substantial in most cases. In this case, inter-stage communication may be feasible only with a 50/50 split ratio in the first scenario with an extra margin of 7 dB beyond the N1 class, or with 20/80% or higher split ratios in the second scenario.

4. CONVERGED COHERENT METRO + PON

Research efforts toward a converged optical network [4,27] aim to reduce costs and enhance flexibility by extending coherent transmission all optically (i.e., without O-E-O conversion) from the metro to the access domain, whether through single-carrier or multi-carrier (i.e., DSCM) approaches, a context

in which our proposed ONU-to-ONU communication fits naturally, as it can meet the low-latency requirements of radio X-hauling while reducing the number of OLTs and central offices. In this section, we therefore propose intra- and inter-PON communication schemes in the context of converged metro–PON setups.

A. Metro + PON Physical Architecture

In a converged metro + PON setup, where the metro and PON segments are interconnected all-optically via reconfigurable optical add–drop multiplexers (ROADMs), three types of connections can be realized: (i) intra-PON communication, established similarly to the architectures discussed in the previous section; (ii) pre-metro connections, where a regular ONU communicates with a node before traversing the metro segment via a ROADM; and (iii) inter-PON communication between ONUs belonging to different PON trees, further enhancing network flexibility and supporting low-latency use cases. We thus discuss here a preliminary link budget analysis for the new cases (ii) and (iii).

In Fig. 7, we show an example of a converged network in which the OLT is located at a remote site and serves several separate PONs connected through different ROADMs (in the figure, for simplicity, we represented only two PON trees). In this configuration, we illustrate both pre-metro and inter-PON connections. For the pre-metro scenario, the connection between the ONUs serving RU1 and DU1 is established using DSCM, where a portion of the signal is dropped at a nearby location (DU1), while the remaining SCs continue toward the metro segment. This functionality is enabled through the addition of three taps connecting the PON tree, the metro, and the pre-metro ONU. The tap that connects the pre-metro ONU to both sides is referred to as the main DU tap. In this example, SCs 11 and 12 are allocated to a bidirectional link between RU1 and DU1. Simultaneously, RU1 maintains its connection to the OLT using SCs 9 and 10, while DU1 uses SCs 13 and 14 for its own OLT connection. Throughout this discussion, as in the previous section, SC numbering is arbitrary and intended solely for illustrative purposes.

For the inter-PON case, a direct all-optical connection between RU2 (from the PON1 tree) and DU2 (from the PON2 tree) is feasible through proper SC planning and the inclusion of optical splitters within the central optical matrix. These splitters enable a mesh-like topology that interconnects PON 1 on the right, PON 2 in the middle, and the OLT on the left. For example, SCs 5 and 6 can establish an inter-PON link between RU2 and DU2, while each site retains OLT connectivity via SCs 7 and 8 (for RU2) and SCs 3 and 4 (for DU2). Meanwhile, standard ONUs in both PONs maintain regular US/DS communication using SCs 15 and 16 in PON 1 and SCs 1 and 2 in PON 2. Here, we assume that the entire set of SCs are dedicated to the PON and switched together in the ROADM. This concept has been presented and discussed in the literature, for example, in studies on filterless operation in ROADMs for horseshoe topologies [28] and metro-PON implementations using DSCM [8]. It is important to highlight that this architecture is compatible with conventional PONs operating at different wavelengths, allowing the proposed connections to be overlaid on existing PON deployments without interfering with ongoing traffic, thereby ensuring flexible and scalable coexistence.

B. Metro + PON First-Order Link Budget Analysis

In the context of the metro + PON setup shown in Fig. 7, the power budget should account not only for previously discussed factors, such as SC power imbalance and acceptable power loss, but also for additional considerations, including the impact of the optical signal-to-noise ratio (OSNR) and filtering effects on the allowable OPL in the PON, as these can further degrade signal quality. These penalties are discussed in [29]

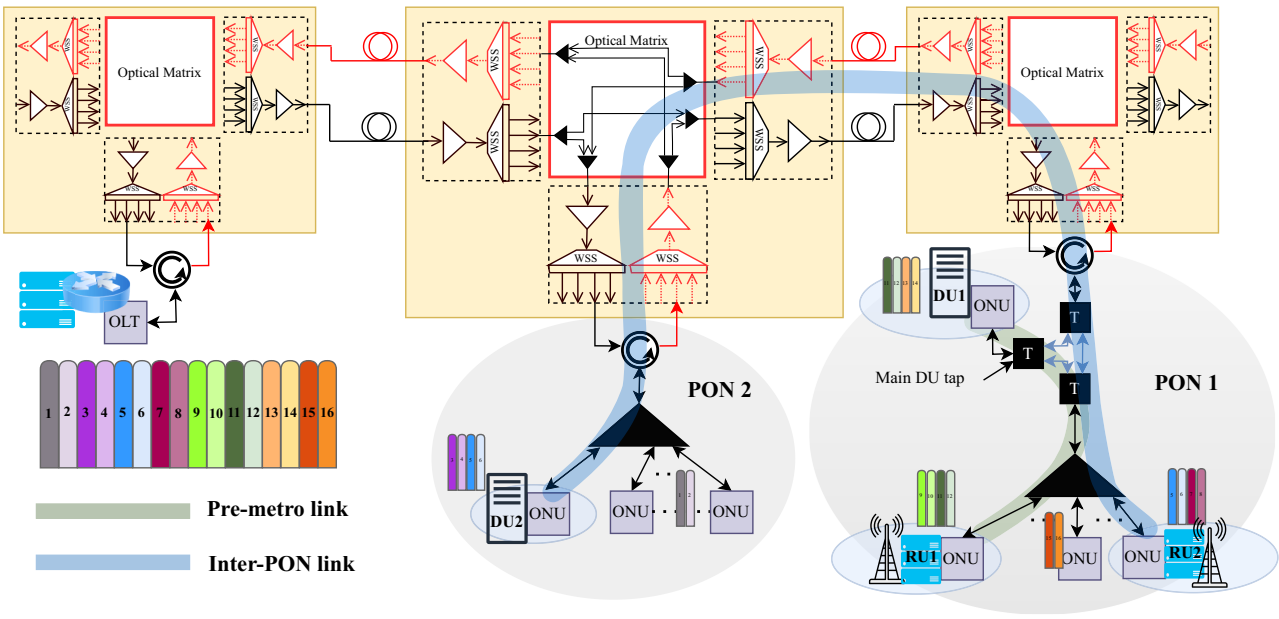

Fig. 7. Pre-metro and inter-PON communications in the coherent DSCM metro + PON setup.

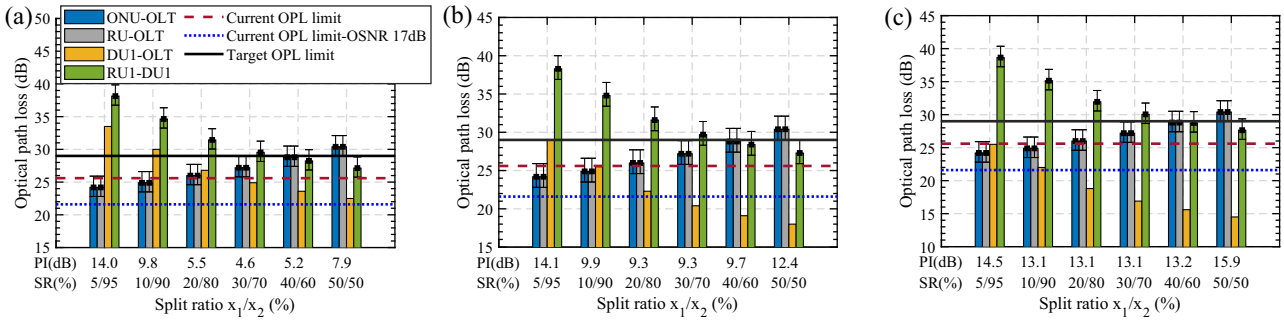

Fig. 8. PON link power budget versus added tap split ratio for a pre-metro link, with DU main tap split ratios of (a) 2/98, (b) 5/95, and (c) 10/90%. The numbers shown below the figures represent the power imbalance for each split ratio. PI, power imbalance; SR, split ratio. The legend in (a) applies to all.

and should be taken into account when planning the physical topology. A detailed analysis of the metro + PON scenario would require a full paper, as it would be significantly more complex than the "single PON tree" studied in the previous section. Consequently, in order to introduce a simple first-order analysis also for this scenario, we neglect filtering effects and assume that an OSNR above 24 dB results in a sensitivity penalty below 0.5 dB, whereas an OSNR of 17 dB incurs a penalty of about 4 dB, thereby reducing the allowable OPL by the same amount. These metro penalty values were reported in [29], based on measurements with a 400 Gbps transceiver using 16 SCs and DP-16-QAM modulation. Accordingly, three OPL thresholds are considered: 29 dB, representing the target N1-class compliant OPL limit; 25.6 dB, corresponding to the current transceivers' OPL limit for links within the PON; and 21.6 dB, applicable to the current transceivers' OPL limit for links traversing the metro segment. The corresponding metro + PON power budget analysis is presented in Fig. 8, with the split ratio of the main DU tap varied across three cases: (a) 2/98, (b) 5/95, and (c) 10/90%. In each case, the first value represents the portion of power directed to the metro segment, and the second represents the portion sent to the PON. For each main tap configuration, the split ratios of the two additional taps (x_1/x_2) are also varied to evaluate the overall power budget of the proposed architecture, where x_1 corresponds to the main PON path and x_2 to the path to and from the pre-metro ONU. The link between RU1 and DU1 must satisfy the PON threshold (i.e., it remains within the PON), whereas the other links must account for the OSNR penalty as they traverse the metro segment to reach their destinations. Results show that the 2/98% main tap split ratio, corresponding to insertion losses of 19 and 0.25 dB, is the most favorable configuration for minimizing power imbalance between DU1–RU1 and DU1–OLT links. This is because the RU1–DU1 path experiences the cumulative loss of two taps plus PON attenuation, whereas the DU1–OLT path passes only two taps before entering the metro. Under the 2/98% main tap configuration shown in Fig. 8(a), the most suitable split ratios for the other two taps are found to be 20/80, 30/70, and 40/60%, as they provide the lowest power imbalance across all links while keeping losses close to the addressed thresholds. Finally, the inter-PON link from DU2 to RU2 is feasible, with an OPL equal to that of the RU–OLT path, while the reverse RU2 to DU2 link experiences a loss equal to the DU2–OLT path.

5. FIRST-ORDER LATENCY ANALYSIS IN THE PROPOSED ARCHITECTURES

In this section, we evaluate the latency reduction enabled by the proposed architectures from a physical perspective, namely, by reducing the physical distance, minimizing O-E-O conversions, and eliminating the need for electrical switching. For the first-order analysis, three factors are considered. The first is the fiber propagation delay, taken as 5 μs/km [10]. The second accounts for transmission protocol delays introduced by O-E-O transceivers, including coding, mapping, error correction, and other digital signal processing functions. In particular, [6] reports a back-to-back latency (including DSP processing) of approximately 31 μs, which we hereafter refer to as the transmitting/receiving (Tx/Rx) latency. Third is the queuing delays incurred in electrical switches, which vary depending on the employed techniques and traffic load. Measurements from the European Advanced Networking Test Center [30] indicate that, for eCPRI-based front-haul traffic between the RU and DU under network congestion with segment routing over IPv6 (SRv6), the minimum and maximum reported latencies for raw front-haul access plus pre-aggregation routers are approximately 20 and 30 μs, respectively.

Within this framework, we compare the latency across three connection types: intra-PON in coherent PON, as illustrated in Fig. 3(a); pre-metro; and inter-PON in a metro + PON configuration, as shown in Fig. 7. For comparison, it is assumed that ONUs are located approximately 20 km from the OLT and 10 km from the splitter in the intra-PON connection. Furthermore, in metro + PON transmission, where traffic passes through ROADMs, the distance between consecutive ROADMs is assumed to be 10 km for simplicity. It is important to note that this comparison focuses solely on the physical-layer latency of all-optical direct links versus conventional links, where the analysis is restricted to physical-layer processes (propagation, O-E-O conversion, and switching) and does not account for dynamic bandwidth allocation or PON higher-layer mechanisms. Table 4 presents the latency comparison results between the proposed and conventional

Table 4. Latency Comparison between Conventional Links and Proposed Direct Optical Connections

Connection Type	Conventional Latency (μs)	Proposed Latency (μs)	Latency Reduction	Notes
Intra-PON	282–292	131	∼54%	Conventional: 2 Tx/Rx, 2 (20 km) fiber links, and switching; proposed: Tx/Rx, (20 km) fiber link.
Pre-metro	382–392	131	∼66%	Conventional: 2 Tx/Rx, 20 km fiber link, 4 (10 km) metro spans, and switching; proposed: Tx/Rx, (20 km) fiber link.
Inter-PON	432–442	281	∼35%	Conventional: 2 Tx/Rx, 2 (20 km) fiber links, 3 (10 km) metro spans, and switching; proposed: Tx/Rx, 2 (20 km) fiber link, and 10 km metro span.

links. For intra-PON communication, the latency of the proposed direct optical link consists solely of Tx/Rx delay and fiber propagation between ONUs. This yields a total of 131 μs ($31 + 2 \times 10 \times 5$ μs). By contrast, conventional O-E-O-based links require two Tx/Rx operations (2×31 μs), two fiber propagations from the ONU to the OLT and back (each 20 km, i.e., $2 \times 20 \times 5$ μs), and an intermediate switching delay of 20–30 μs. The resulting latency of 282–292 μs is more than twice that of the proposed solution, corresponding to a reduction of approximately 54%. In the pre-metro scenario, the conventional path includes a 20 km ONU–OLT fiber segment, four additional 10 km metro fiber spans back and forth, an intermediate switching stage, and a second Tx/Rx conversion, resulting in a latency of 382–392 μs ($20 \times 5 + 4 \times 10 \times 5 + 2 \times 31 + (20 - 30)$). In contrast, the proposed approach requires only one Tx/Rx operation and a 20 km ONU–ONU fiber link, yielding 131 μs. This corresponds to a reduction of 251–261 μs, or approximately 66%. Lastly, for inter-PON connectivity, the conventional link entails a Tx/Rx delay twice (2×31 μs), propagation from the ONU to the ROADM (20×5 μs), three intermediate hops totaling $3 \times 10 \times 5$ μs, additional propagation from the ROADM to the ONU (20×5 μs), and switching delays of 20–30 μs. This yields a latency of 430–440 μs. In contrast, the proposed direct optical link requires only a single Tx/Rx operation (31 μs) and an ONU to ROADM (100 μs), one metro span (50 μs), ROADM to ONU (100 μs), yielding 281 μs. This corresponds to a reduction of about 35%. The observed reductions range from 35% to over 50%, depending on the configuration and link type. Overall, the results indicate that the proposed all-optical transmission scheme substantially decreases end-to-end latency by eliminating O-E-O conversions and minimizing switching stages in both coherent PONs and converged metro + PON networks.

6. CONCLUSION

We proposed simple physical modifications to the PON infrastructure combined with coherent DSCM to effectively enable both intra- and inter-PON ONU-to-ONU communication without relying on O-E-O conversion at the OLT. Such direct, all-optical connectivity offers a backward-compatible upgrade path for coherent PON and metro + PON systems to support the evolving demands of ultra-high bitrates and stringent latency in future X-haul networks. Our results show that future compliant transceivers require a minimum of 1.3 dB of additional loss margin beyond the 29 dB N1 PON class limit to support a 40 km ONU-to-ONU connection. We also demonstrated the role of optimal split ratio options in managing link budgets and minimizing power imbalances between SCs while confirming the latency advantages of bypassing the OLT in intra- and inter-PON traffic. Future work will focus on defining and solving the split ratio optimization problem for each PON deployment scenario to enable both traditional and ONU-to-ONU communications, as well as providing an experimental proof-of-concept demonstration for latency and power analysis.

Funding. HORIZON EUROPE Marie Sklodowska-Curie Actions (101073265).

Acknowledgment. This work has received funding from the European Union's Horizon Europe research and innovation program under the Marie Skłodowska-Curie grant agreement no. 101073265 (EWOC; for further info, see [13]). Views and opinions expressed are, however, those of the authors only and do not necessarily reflect those of the European Union. The European Union cannot be held responsible for them. A large part of the background research leading to this paper derives from experimental activities carried out in the PhotoNext Center at Politecnico di Torino.

Disclosures. The authors declare no conflicts of interest.

REFERENCES

1. R. Gaudino, "Coherent PON: recent evolutions and expected trends," in *Optical Fiber Communication Conference (OFC)* (2025), paper M2I.1.
2. Z. Jia, H. Zhang, K. Choutagunta, *et al.*, "Coherent passive optical network: applications, technologies, and specification development [Invited Tutorial]," J. Opt. Commun. Netw. **17**, A71–A86 (2025).
3. T. Pfeiffer, P. Dom, S. Bidkar, *et al.*, "PON going beyond FTTH [Invited Tutorial]," J. Opt. Commun. Netw. **14**, A31–A40 (2022).
4. G. Rizzelli, M. Casasco, V. Ferrero, *et al.*, "Analysis and experimental demonstration of possible architectures for future coherent metro+PON converged networks [Invited]," J. Opt. Commun. Netw. **17**, A142–A154 (2025).
5. F. Saliou, P. Chanclou, G. Simon, *et al.*, "Optical access networks to support future 5G and 6G mobile networks [Invited]," J. Opt. Commun. Netw. **17**, C22–C29 (2025).
6. G. Simon, F. Saliou, A. Afonso, *et al.*, "200 Gb/s coherent point-to-multipoint coexistence with 50G-PON for next-generation optical access," IEEE Photonics Technol. Lett. **36**, 665–668 (2024).
7. T. Duthel, C. R. Fludger, B. Liu, *et al.*, "DSP design for coherent optical point-to-multipoint transmission," J. Lightwave Technol. **42**, 1109–1118 (2024).
8. Y. Hu, A. Yan, J. Zhao, *et al.*, "All-optical metro-access integration network bidirectional transmission enabled by coherent digital subcarrier multiplexing," J. Opt. Commun. Netw. **17**, 58–70 (2025).
9. A. Larrañaga, S. Lagén, J. M. Fàbrega, *et al.*, "Fronthaul/midhaul networks: capacity and latency requirements imposed by 6G disaggregated RANs," IEEE Commun. Mag. **63**(5), 86–93 (2025).

10. T. Pfeiffer, "Considerations on transport latency in passive optical networks," in *45th European Conference on Optical Communication (ECOC)* (2019).
11. J. Maes, S. Bidkar, M. Straub, *et al.*, "Efficient transport of enhanced CPRI fronthaul over PON [Invited]," J. Opt. Commun. Netw. **16**, A136–A142 (2024).
12. S. Das, F. Slyne, A. Kaszubowska, *et al.*, "Virtualized EAST–WEST PON architecture supporting low-latency communication for mobile functional split based on multiaccess edge computing," J. Opt. Commun. Netw. **12**, D109–D119 (2020).
13. Z. Vujicic, M. C. Santos, R. Méndez, *et al.*, "Toward virtualized optical-wireless heterogeneous networks," IEEE Access **12**, 87776–87806 (2024).
14. 3GPP, "Study on new radio access technology: radio access architecture and interfaces (release 14)," Tech. Rep. TR 38.801 V14.0.0 (2017).
15. 3GPP, "Study on CU-DU lower layer split for NR; (release 15)," Tech. Rep. TR 38.816 V15.0.0 (2017).
16. J. Pérez-Romero, O. Sallent, A. Gelonch, *et al.*, "A tutorial on the characterisation and modelling of low layer functional splits for flexible radio access networks in 5G and beyond," IEEE Commun. Surv. Tutorials **25**, 2791–2833 (2023).
17. O-RAN Open Xhaul Transport Working Group 9, "Xhaul transport requirements," Tech. Rep. O-RAN.WG9.XTRP-REQ-v01.00 (O-RAN Alliance, 2021).
18. Broadband Forum, "G-PON & XG-PON & XGS-PON interoperability test plan," Tech. Rep. TP-255 Issue 2 (2024), https://www.broadband-forum.org/pdfs/tp-255-2-0-0.pdf.
19. P. Torres-Ferrera, J. Sime, T. Duthel, *et al.*, "Single-fiber bidirectional transmission using 400G coherent digital subcarrier transceivers," in *Optical Fiber Communication Conference (OFC)* (2024), paper Tu3E.5.
20. G. Rizzelli, G. Bosco, D. Pilori, *et al.*, "Next generation coherent PONs: technical challenges and outlook," in *24th International Conference on Transparent Optical Networks (ICTON)* (2024).
21. H. Zhang, Z. Jia, L. A. Campos, *et al.*, "Hybrid TFDM coherent PON featuring adaptable capacity and out-of-band communication channels," in *Optical Fiber Communication Conference (OFC)* (2024), paper Th1E.6.
22. J. Zhou, Z. Xing, H. Wang, *et al.*, "Flexible coherent optical access: architectures, algorithms, and demonstrations," J. Lightwave Technol. **42**, 1193–1202 (2024).
23. J. Li, R. Fan, Q. He, *et al.*, "Bidirectional TFDM 200 G coherent PON with a simplified receiver at the ONU side," Opt. Lett. **49**, 5127–5130 (2024).
24. "Go4fiber singlemode coupler/splitter/tap specifications" [accessed 21 July 2025], https://spec.go4fiber.com/coupler_wdm/Singlemode_Coupler_Tap_2018v1.pdf.
25. "1x3, 1x4, 1x5 singlemode coupler/tap (equal split) specifications" [accessed 21 July 2025], https://spec.go4fiber.com/coupler_wdm/1x3_1x4_1x5_SM_coupler_tap_2021v1.pdf.
26. G. Simon, P. Chanclou, F. Saliou, *et al.*, "Clustering G-PON field data to improve flexibility in next generation PON systems," in *European Conference on Optical Communication (ECOC)* (2021).
27. G. Rizzelli, M. Casasco, E. Riccardi, *et al.*, "Experimental investigation on the fundamental physical-layer capabilities for converged metro–access architectures using coherent transceivers," J. Opt. Commun. Netw. **17**, 648–658 (2025).
28. M. M. Hosseini, J. Pedro, A. Napoli, *et al.*, "Optimization of survivable filterless optical networks exploiting digital subcarrier multiplexing," J. Opt. Commun. Netw. **14**, 586–594 (2022).
29. P. Torres-Ferrera, G. Parisi, J. Sime, *et al.*, "Experimental verification of an analytical model of filtering impact on coherent digital subcarriers systems," in *Optical Fiber Communication Conference (OFC)* (2025), paper Th2A.21.
30. "5G xHaul design with SRv6" EANTC [accessed 17 August 2025], https://wiki.eantc.de/wiki/publicreports/view/Main/Multi-Vendor%20MPLS%20%26%20SDN%20Interoperability%20Test%20Report%202025/SRv6/5G%20xHaul%20design%20with%20SRv6.